Superscaling in electron-nucleus scattering and its link to CC and NC QE neutrino-nucleus scattering

M.B. Barbaro*, J.E. Amaro†, J.A. Caballero**, T.W. Donnelly‡, R. González-Jiménez**, M. Ivanov§ and J.M. Udías¶

* *Università di Torino and INFN, Sezione di Torino, 10125 Torino, ITALY*
† *Universidad de Granada, 18071 Granada, SPAIN*
** *Universidad de Sevilla, 41080 Sevilla, SPAIN*
‡ *CTP, LNS and Department of Physics, MIT, Cambridge, MA 02139, USA*
§ *Institute for Nuclear Research and Nuclear Energy, Sofia 1784, BULGARIA*
¶ *Universidad Complutense de Madrid, 28040 Madrid, SPAIN*

Abstract. The superscaling approach (SuSA) to neutrino-nucleus scattering, based on the assumed universality of the scaling function for electromagnetic and weak interactions, is reviewed. The predictions of the SuSA model for bot CC and NC differential and total cross sections are presented and compared with the MiniBooNE data. The role of scaling violations, in particular the contribution of meson exchange currents in the two-particle two-hole sector, is explored.

Keywords: Neutrino interactions; SuperScaling; Quasielastic scattering; Meson exhcange currents.
PACS: 25.30.Pt, 13.15.+g, 24.10.Jv

Several theoretical models have been developed in recent years in order to describe neutrino and antineutrino quasielastic (QE) scattering [1, 2, 3, 4, 5, 6, 7]. The obvious test for a model to be used in the description of QE neutrino reactions is the comparison with all the available electron scattering data at similar kinematics. With this motivation, the Superscaling approximation (SuSA) model, which *uses* the best world data for electron scattering to predict neutrino cross section, was proposed in Ref. [8].

The model is based on the superscaling properties of QE inclusive electron scattering data [9, 10, 11, 12], namely the simultaneous independence of the reduced (e,e') cross section upon the momentum transfer q (first-kind scaling) and nuclear target (second-kind scaling) when represented as a function of an appropriate scaling variable ψ'. It clearly emerges from the analysis represented in Fig. 1 that the relativistic Fermi gas (RFG) model gives a very poor description of the data, failing to reproduce both the size and the shape of the experimental superscaling function. The predictions for neutrino-nucleus cross sections are then simply obtained by multiplying the phenomenological superscaling function f by the corresponding elementary weak cross sections. The model reproduces by construction the longitudinal electron scattering response at all kinematics and for all nuclei.

Beyond agreeing by definition (up to scaling violations to be discussed later) with electron scattering data, the model has other merits. First, it accounts for both kinematical and dynamical relativistic effects, which have been shown to be relevant even at moderate momentum and energy transfers [13, 14]. As a consequence the model can be safely used in a wide energy range, from the MiniBooNE typical conditions ($E_\nu \simeq 0.7$ GeV) up to several GeV neutrino experiments as NOMAD [15]. Second, due to second-kind scaling, it allows for a consistent treatment of different target nuclei, which is particularly interesting for the MINERvA experiment [16]. Finally, the SuSA model can be extended to non-QE kinematics, which is not the focus of this presentation (see Refs. [8, 17, 18]).

On the other hand the main limitation of the SuSA approach arises from the fact that it neglects scaling violations. These occur mainly in the transverse channel at energies above the QE peak and are associated to non-impulsive effects, like inelastic scattering and meson-exchange currents (MEC).

The latter are two-body currents carried by a virtual meson exchanged between two bound nucleons. They can excite both 1p1h and 2p2h states. In the 1p1h sector, studies of electromagnetic (e,e') process have shown that the MEC, when combined with the corresponding correlations, which are needed to preserve gauge invariance, give a small contribution to the QE cross section and can be neglected in first approximation. In the 2p2h sector, however, MEC are known to give a significant positive contribution to the (e,e') cross section at high energy transfers, leading to a partial filling of the "dip" between the QE and Δ-resonance peaks. This region is relevant for the MiniBooNE experiment, where "QE" events (namely with no real pions in the final state) can involve transferred energies far

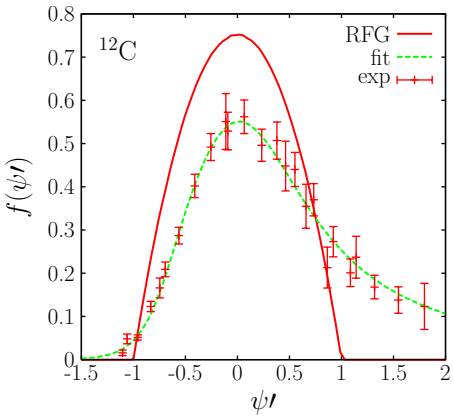

FIGURE 1. The experimental superscaling function f displayed versus the scaling variable ψ' (see Ref. [8] for definitions) and compared with the RFG result.

beyond the QE peak, due to the large energy range spanned by the neutrino flux. Such 2p2h mechanisms were indeed proposed in Refs. [5, 6] as a possible explanation of the "axial mass puzzle", namely the fact that the recent CCQE and NCQE MiniBooNE results [19, 20, 21] turn out to be substantially underestimated by the RFG prediction, unless an unusually large *ad hoc* value of the axial mass $M_A \simeq 1.35$ GeV/c^2 (as compared to the standard value $M_A \simeq 1$ GeV/c^2) is employed in the dipole parametrization of the nucleon axial form factor. Notably also the relativistic Green's function model, based on a particular treatment of final state interaction [22] through a phenomenological optical potential, can reasonably reproduce the MiniBooNE data, indicating that contributions beyond the simple IA play an important role in QE neutrino reactions at MiniBooNE kinematics.

Our approach to MEC, developed for use in electron scattering reactions (see Refs. [23, 24]), is fully relativistic and takes into account all the 2p2h many-body diagrams corresponding to the two-body current in Fig. 2. In order to apply the model to neutrino scattering, we observe that in lowest order the 2p2h sector is not directly reachable for the axial-vector matrix elements. Hence at this order the MEC affect only the transverse polar vector response.

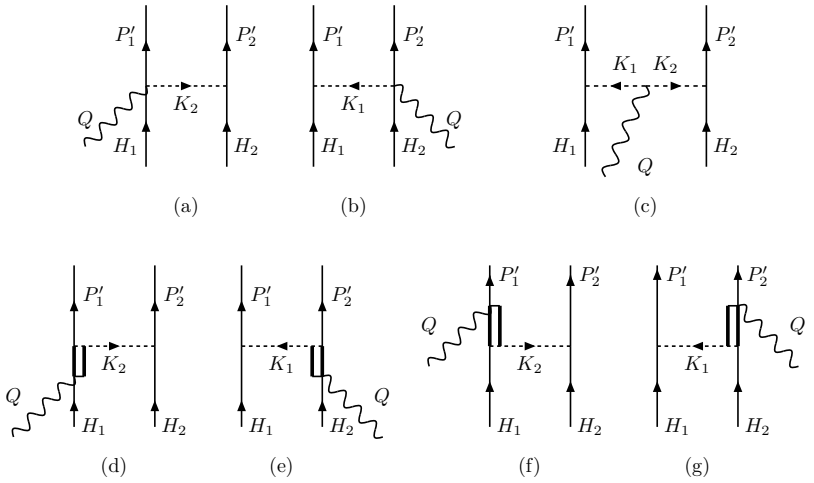

FIGURE 2. Two-body meson-exchange currents. (a) and (b): "contact", or "seagull" diagram; (c): "pion-in-flight" diagram; (d)-(g): "Δ-MEC" diagram. Dashed lines represent pions, thin lines nucleon and thick lines represent the propagation of the Δ-resonance.

The results of the SuSA model for the double differential CCQE neutrino and antineutrino cross sections are shown in Figs. 3: they appear to fall below the neutrino data for most of the angle and energy bins. Note that we do not compare with the most forward angles ($0.9 < \cos\theta < 1$) since for such kinematics roughly 1/2 of the cross section has been proved [25] to arise from very low excitation energies (<50 MeV), where the cross section is dominated by collective excitations and any approach based on IA is bound to fail.

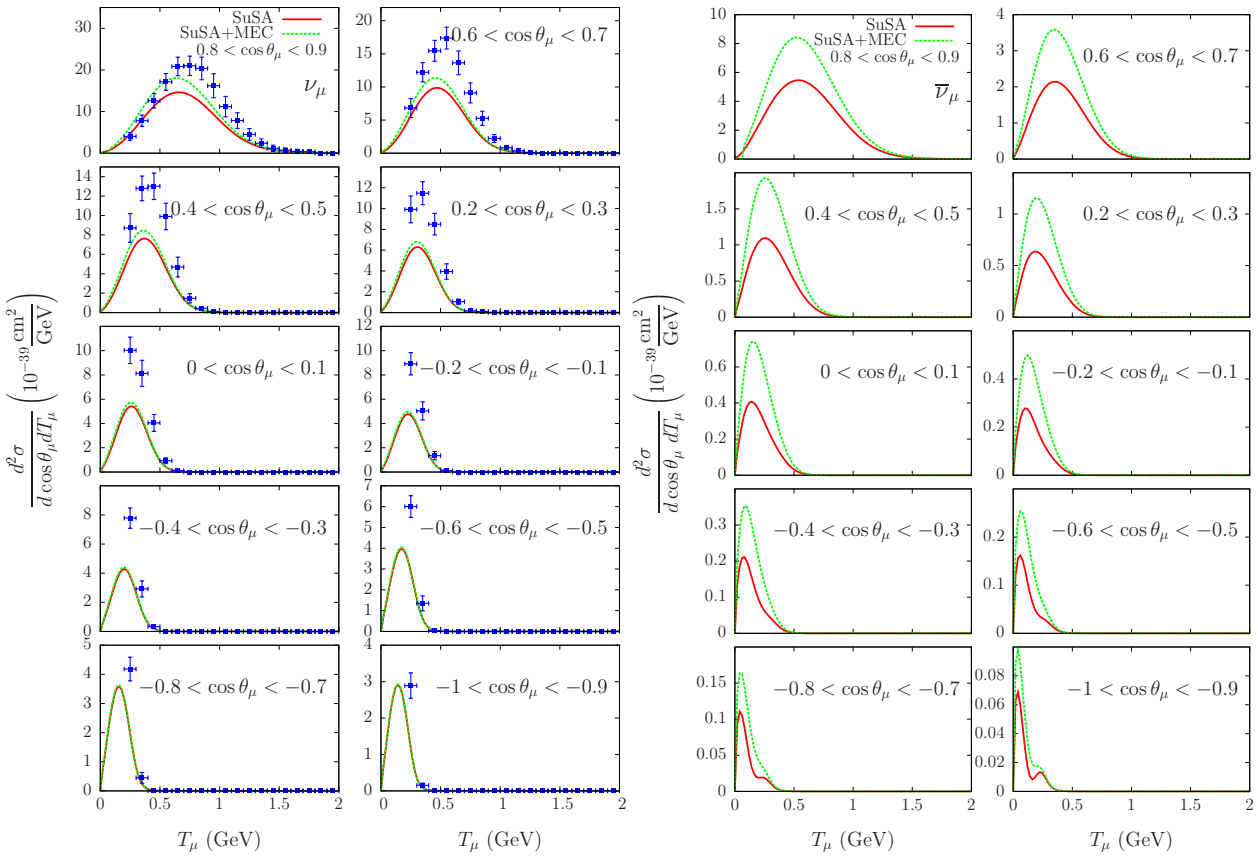

FIGURE 3. Flux-averaged ν_μ-^{12}C (left) and $\overline{\nu}_\mu$-^{12}C (right) CCQE double differential cross sections per target nucleon evaluated in the SuSA model with and without inclusion of 2p2h MEC and in the RMF model and displayed versus the muon kinetic energy T_μ for various bins of the muon scattering angle $\cos\theta$. Neutrino data are from MiniBooNE [19].

The inclusion of 2p2h MEC yields larger cross sections and accordingly better agreement with the neutrino data, but theory still lies below the data at larger angles where the cross sections are smaller. It should be noted, however, that the present approach still lacks the contributions from the correlation diagrams associated with the MEC which are required by gauge invariance, and these might improve the agreement with the data.

Predictions for antineutrino cross section are also shown, which can be compared with the new antineutrino data from MiniBooNE [20]. Note that in our model, due to the interplay between the vector and axial-vector responses in the total cross section, the effect of MEC is larger than for the neutrino case.

In Fig. 4 we display the SuSA results for the total cross sections. In the neutrino case we also show the results obtained in the relativistic mean field (RMF) model, which are very close to the SuSA ones. The RFM represents in fact a microscopic justification of the phenomenological superscaling approach: as shown in Ref. [1], it is able to reproduce the asymmetric shape of the superscaling function, a feature hardly described by other microscopic models.

In Ref. [29] the SuSA model has been applied to the neutral current (NC) process with both neutrinos and antineutrinos and the results have been compared with the MiniBooNE data on CH_2 [21]. The results are shown in Fig. 5 as functions of the "quasi-elastic" four-momentum transfer Q_{QE} defined in [21]. We note that the SuSA cross section is smaller than the RFG one by about 20% and the two curves have essentially the same slope in Q^2. On the other hand the RMF result has a softer Q^2 behavior, with a smaller slope. This is at variance with the CCQE case, for which, as shown in Ref. [27], SuSA and RMF cross sections are very close to each other. This result indicates, as expected, that the NC data, for which the outgoing nucleon is detected, are more sensitive to the different treatment of final-state interactions than the MiniBooNE CC data, where the ejected nucleon is not observed.

It is well-known (see, *e.g.*, [32, 31]) that the $g_A^{(s)}$-dependence of the NCQE neutrino-nucleon cross section is very

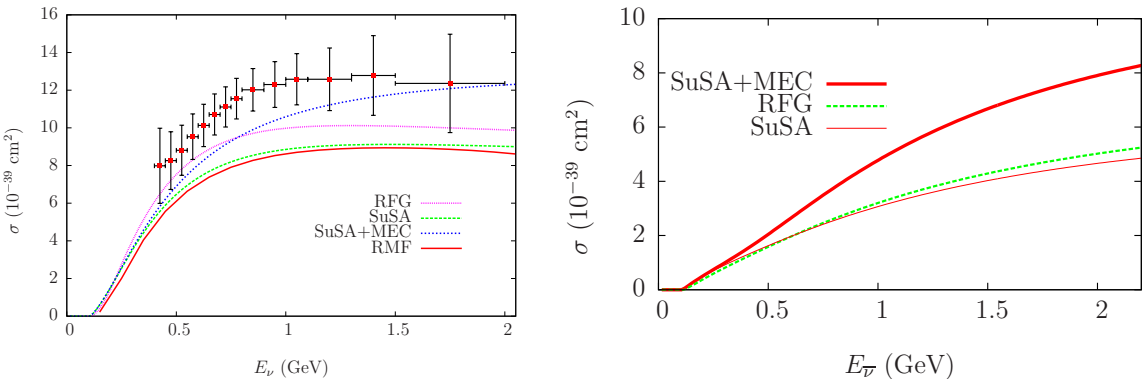

FIGURE 4. Flux-averaged ν_μ-^{12}C (left) and $\overline{\nu}_\mu$-^{12}C (right) CCQE cross section integrated over the muon kinetic energy and scattering angle and displayed versus the unfolded neutrino energy. Data from Ref. [19].

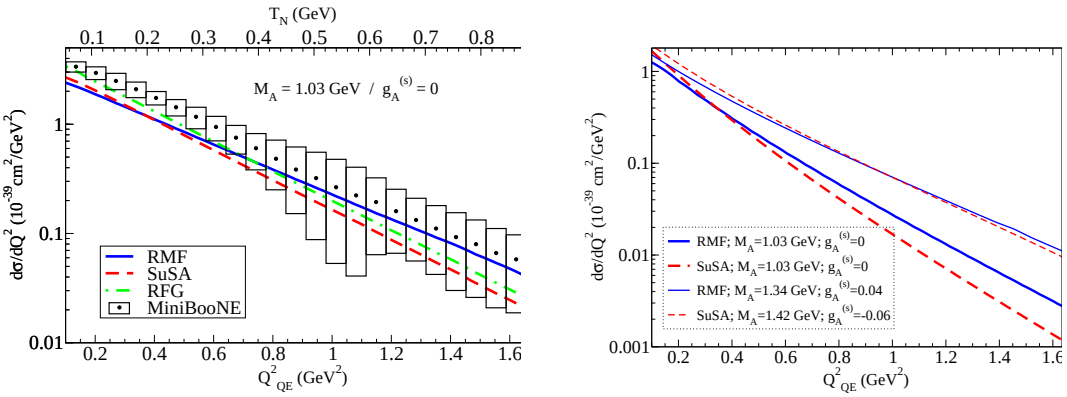

FIGURE 5. NCQE flux-averaged neutrino (left) and antineutrino (right) cross section off CH_2 compared with the MiniBooNE data [21].

mild, but the proton/neutron cross sections ratio is instead very sensitive to variations of the strange axial form factor. The MiniBooNE experiment cannot measure the p/n ratio because the $\nu n \to \nu n$ reaction cannot be isolated. However, single-proton events have been isolated and the ratio $(\nu p \to \nu p)/(\nu N \to \nu N)$ has been reported in Ref. [21] as a function of the reconstructed nucleon kinetic energy $T_{\rm rec}$ from 350 to 800 MeV. In Fig. 6 we compare the experimental ratio with the predictions of the SuSA model for the standard values of M_A and $g_A^{(s)}$ and for a set of parameters corresponding to a χ^2 fit to the axial strangeness parameter. As expected, the ratio, unlike the cross section, is sensitive to axial strangeness, and the SuSA predictions are in good agreement with the data within the experimental error.

Summarizing, we have shown that the superscaling model, which by construction describes with excellent accuracy the QE (e,e') data in the scaling region, can be applied to the study of both CC and NC neutrino reactions. The model is relativistic and can therefore be used up to several GeV neutrino energies. Moreover it can be used to describe the response of different nuclear targets to electroweak probes.

Comparison with the MiniBooNE neutrino data shows that, if the standard value of the nucleon axial mass is used, the model underestimates the experimental cross sections. The inclusion of 2p2h MEC contributions, which violate superscaling and must be added to the model, increases both the differential and the integrated cross sections and thus seems to improve the agreement with the data. However, in the present scheme, more refined calculations taking care of correlation currents and MEC effects in the axial-vector channel should be performed before final conclusions can be drawn. We refer the reader to the bibliography for further details and results.

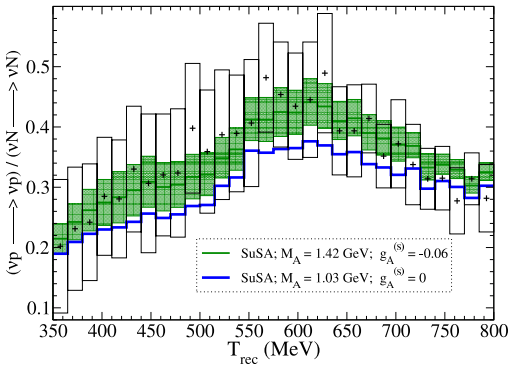

FIGURE 6. Ratio $(\nu p \to \nu p)/(\nu N \to \nu N)$ computed within the SuSA model. Shadowed areas represent the 1-σ region allowed for $g_A^{(s)}$. The ratio computed with the best-$g_A^{(s)}$ is presented as well as those obtained with the standard axial mass and no strangeness. Data from Ref. [21].

REFERENCES

1. J. A. Caballero, J. E. Amaro, M. B. Barbaro, T. W. Donnelly, C. Maieron and J. M. Udias, Phys. Rev. Lett. **95**, 252502 (2005).
2. T. Leitner, L. Alvarez-Ruso and U. Mosel, Phys. Rev. C **73**, 065502 (2006).
3. J. E. Amaro, M. B. Barbaro, J. A. Caballero, T. W. Donnelly and J. M. Udias, Phys. Rev. C **75**, 034613 (2007).
4. O. Benhar, P. Coletti and D. Meloni, Phys. Rev. Lett. **105**, 132301 (2010).
5. M. Martini, M. Ericson, G. Chanfray and J. Marteau, Phys. Rev. C **81**, 045502 (2010).
6. J. Nieves, I. Ruiz Simo and M. J. Vicente Vacas, Phys. Rev. C **83**, 045501 (2011).
7. A. Meucci, M. B. Barbaro, J. A. Caballero, C. Giusti and J. M. Udias, Phys. Rev. Lett. **107**, 172501 (2011).
8. J. E. Amaro, M. B. Barbaro, J. A. Caballero, T. W. Donnelly, A. Molinari and I. Sick, *Phys. Rev.* **C71** 015501 (2005).
9. W. M. Alberico, A. Molinari, T. W. Donnelly, E. L. Kronenberg and J. W. Van Orden, Phys. Rev. C **38**, 1801 (1988).
10. D. B. Day, J. S. McCarthy, T. W. Donnelly and I. Sick, Ann. Rev. Nucl. Part. Sci. **40**, 357 (1990).
11. T. W. Donnelly and I. Sick, Phys. Rev. Lett. **82**, 3212 (1999).
12. T. W. Donnelly and I. Sick, Phys. Rev. C **60**, 065502 (1999).
13. J. E. Amaro, M. B. Barbaro, J. A. Caballero, T. W. Donnelly and A. Molinari, Nucl. Phys. A **643**, 349 (1998).
14. J. E. Amaro, M. B. Barbaro, J. A. Caballero, T. W. Donnelly and A. Molinari, Phys. Rept. **368**, 317 (2002).
15. VLyubushkin *et al.* [NOMAD Collaboration], Eur. Phys. J. C **63**, 355 (2009).
16. G. Fiorentini, these Proceedings.
17. C. Maieron, J. E. Amaro, M. B. Barbaro, J. A. Caballero, T. W. Donnelly and C. F. Williamson, Phys. Rev. C **80**, 035504 (2009).
18. M. V. Ivanov, J. M. Udias, A. N. Antonov, J. A. Caballero, M. B. Barbaro and E. M. de Guerra, Phys. Lett. B **711**, 178 (2012).
19. A. A. Aguilar-Arevalo *et al.* [MiniBooNE Collaboration], *Phys. Rev.* **D81** 092005 (2010).
20. A. A. Aguilar-Arevalo *et al.* [MiniBooNE Collaboration], arXiv:1301.7067 [hep-ex].
21. A. A. Aguilar-Arevalo *et al.* [MiniBooNE Collaboration], Phys. Rev. D **82**, 092005 (2010).
22. A. Meucci, these proceedings.
23. A. De Pace, M. Nardi, W. M. Alberico, T. W. Donnelly and A. Molinari, Nucl. Phys. A **726**, 303 (2003) [nucl-th/0304084].
24. A. De Pace, M. Nardi, W. M. Alberico, T. W. Donnelly and A. Molinari, Nucl. Phys. A **741**, 249 (2004) [nucl-th/0403023].
25. J. E. Amaro, M. B. Barbaro, J. A. Caballero, T. W. Donnelly and C. F. Williamson, *Phys. Lett.* **B696** 151 (2011).
26. J. E. Amaro, M. B. Barbaro, J. A. Caballero and T. W. Donnelly, Phys. Rev. Lett. **108**, 152501 (2012).
27. J. E. Amaro, M. B. Barbaro, J. A. Caballero, T. W. Donnelly and J. M. Udías, *Phys. Rev.* **D84** 033004 (2011).
28. J. E. Amaro, C. Maieron, M. B. Barbaro, J. A. Caballero and T. W. Donnelly, *Phys. Rev.* **C82** 044601 (2010).
29. R. Gonzalez-Jimenez, M. V. Ivanov, M. B. Barbaro, J. A. Caballero and J. M. Udias, Phys. Lett. B **718**, 1471 (2013).
30. J. E. Amaro, M. B. Barbaro, J. A. Caballero and T. W. Donnelly, Phys. Rev. C **73**, 035503 (2006).
31. W. M. Alberico, M. B. Barbaro, S. M. Bilenky, J. A. Caballero, C. Giunti, C. Maieron, E. Moya de Guerra and J. M. Udias, Nucl. Phys. A **623**, 471 (1997).
32. M. B. Barbaro, A. De Pace, T. W. Donnelly, A. Molinari and M. J. Musolf, Phys. Rev. C **54**, 1954 (1996).